ASTM INTERNATIONAL

Geotechnical Testing Journal

H. Shen,[1] W. Haegeman,[2] and H. Peiffer[3]

DOI: 10.1520/GTJ20150149

# 3D Printing of an Instrumented DMT: Design, Development, and Initial Testing

Geotechnical Testing Journal

doi:10.1520/GTJ20150149 available online at www.astm.org

# TECHNICAL NOTE

H. Shen,[1] W. Haegeman,[2] and H. Peiffer[3]

# 3D Printing of an Instrumented DMT: Design, Development, and Initial Testing

**Reference**

Shen, H., Haegeman, W., and Peiffer, H., "3D Printing of an Instrumented DMT: Design, Development, and Initial Testing," *Geotechnical Testing Journal* doi:10.1520/GTJ20150149. ISSN 0149-6115

**ABSTRACT**

This paper describes the design, fabrication, and initial testing of an instrumented flat dilatometer test (iDMT) device. Compared to the DMT test involving pressure readings at two fixed displacements, this device is designed to have a direct displacement-measuring system and a larger displacement range to evaluate the continuous pressure-displacement relation of a soil, which may afford an opportunity to improve the interpretation to take non-linear soil behaviors into account rather than using linear elasticity in the DMT analysis. However, technical constraints are encountered in the iDMT blade machining using traditional technologies; alternatively, a 3D printing technology is successfully applied to fabricate the iDMT blade. Then, the calibrations of the iDMT device are performed, followed by an iDMT test in conjunction with a DMT test in a calibration chamber, demonstrating that the new iDMT device can be used to investigate non-linear soil behaviors, and the 3D printing technology is proved not only to be an expedient solution but also to be used as a routine tool in improving geotechnical testing apparatus.

**Keywords**

DMT, instrumented DMT, 3D printing, pressures, displacement

Manuscript received July 7, 2015; accepted for publication January 15, 2016; published online March 8, 2016.

[1] Ph.D. Candidate, Laboratory of Geotechnics, Ghent Univ., Technologiepark 905, B-9052 Zwijnaarde, Belgium (Corresponding author), e-mail: shenhao.geo@gmail.com

[2] Professor, Laboratory of Geotechnics, Ghent Univ., Technologiepark 905, B-9052 Zwijnaarde, Belgium, e-mail: wim.haegeman@ugent.be

[3] Professor, Laboratory of Geotechnics, Ghent Univ., Technologiepark 905, B-9052 Zwijnaarde, Belgium, e-mail: herman.peiffer@ugent.be

## Introduction

The flat dilatometer test (DMT), introduced by Marchetti, has become a routine in situ testing device, which can provide highly reproducible and reliable soil properties (Marchetti 1980; Marchetti et al. 2001; Schnaid 2009). The DMT measures pressures at two center displacements of the membrane: 0.05 mm and 1.1 mm. Then intermediate dilatometer parameters are defined and employed to interpret soil properties. For instance, the dilatometer modulus $E_d$ can be obtained

using linear elasticity. However, it is necessary to recognize non-linearity of soil stiffness, this stiffness changes with the strain in soils by orders of magnitude, so the prediction of a modulus can only be accurate if the strain in a soil is appropriate to the strain relevant to the $E_d$. Thus, it appears interesting to adjust the DMT to be able to investigate the in situ non-linear soil behavior by providing a direct displacement measurement and a sufficiently large displacement range.

Various modifications of the DMT have been proposed for different purposes (Shen et al. 2015). With the aim of better understanding of the DMT, continuous displacement measurements, from 0 to 1.1 mm/1.0 mm, and pressure measurements have been introduced (Campanella and Robertson 1991; Fretti et al. 1992; Akbar and Clarke 2001; Stetson et al. 2003). Either a flexible steel membrane or a rigid piston is used as the loading element, a linear pressure-displacement relationship is typically found from these modified DMTs. The non-linear pressure-displacement relation is only found in the modified DMT featured by a piston expansion of 3 mm and a non-instrumented blade (Colcott and Lehane 2012). Specifically, the piston is expanded by a manually controlled hydraulic system, and the piston displacement is indirectly determined by measuring the volume change of the pumped oil, which may bring a number of potential sources of error.

To overcome the aforementioned issues presented in the literature, a new iDMT blade was fabricated with an electrical computer control system and a direct displacement-measuring system to remove the error inherent in the manual control, as well as the inference of displacement from the volume of pressurized fluid. However, the prototype was not successfully produced in traditional subtractive manufacturing, as the blade machining was found technically difficult concerning a mere 15 mm of blade thickness together with a sufficiently large expansion, such as a 3-mm piston expansion (Colcott and Lehane 2012), to evaluate non-linear soil behaviors. 3D printing, a term used synonymously with additive manufacturing, creates an object adding material layer by layer, which then provides opportunities to fabricate objects that are impossible for traditional subtractive manufacturing (ASTM F2792-12a 2012; Christopher 2014). Although the 3D printing technology already has a number of groundbreaking applications in many fields, it is surprising to see its limited uses in geotechnical testing, as one may have the incorrect impression that 3D printing products are not robust enough to withstand the pressure required for geotechnical testing. This paper aims to alter this judgment by presenting a novel iDMT development with the following specific objectives:

1. Non-linear soil behaviors can be taken into account by a sufficiently large displacement of the piston.
2. Continuous pressure and displacement measurements are recorded automatically.
3. A comparison with the standard DMT test results is allowed to evaluate the iDMT.
4. The design is fabricable using 3D printing technology.

## Design and Fabrication

### INSTRUMENTED DMT BLADE DESIGN

**Fig. 1** illustrates 3D models of the iDMT blade generated in a CAD-software along with the assemble diagram. The design (**Fig. 1(a)**) involves a main iDMT blade body, a piston and two removable covers in 3D printed material alumide and other

**FIG. 1**

Schematic CAD-generated diagrams of the instrumented DMT blade: (a) preassembly, (b) assembly in the top view, and (c) assembly in the bottom view.

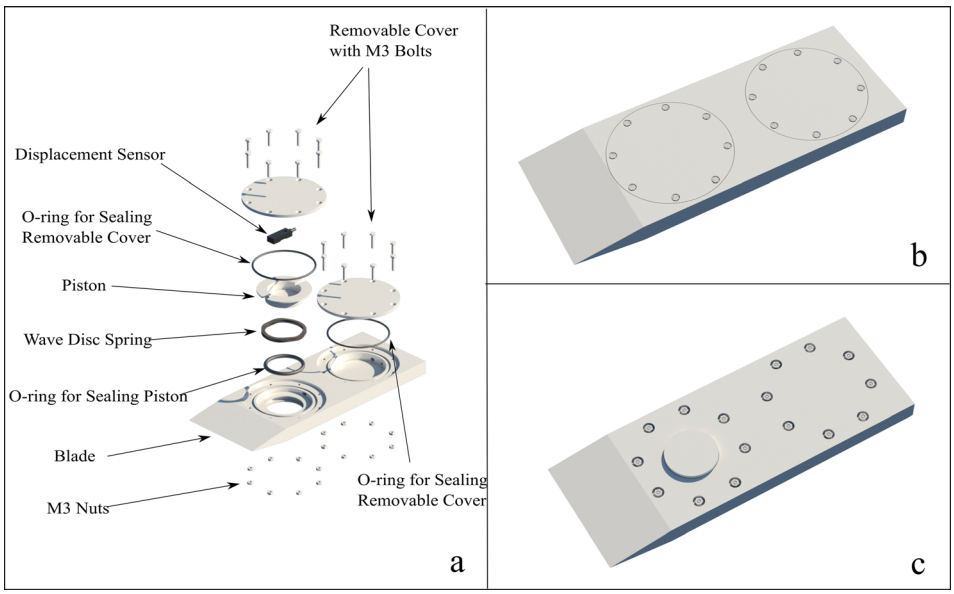

**TABLE 1** Main properties of alumide (EOS 2012).

| Density (kg/m3) | Tensile Modulus (MPa) | Tensile Strength (MPa) | Flexural Strength (MPa) | Flexural Modulus (MPa) | Strain at Break (%) |
|---|---|---|---|---|---|
| 1360 | 3800 | 48 | 72 | 3600 | 4 |

components in various materials. Specifically, the design uses a 40-mm diameter piston instead of a 60-mm diameter flexible steel membrane. Using a rigid piston in the modified DMTs has been investigated, showing that a piston is more robust than a membrane especially when the displacement goes larger (Akbar and Clarke 2001; Colcott and Lehane 2012). Different from the previous modified DMTs using a piston, an expansion of 6.205 % of the piston diameter is allowed in this design having a 40-mm diameter together with a 2.48-mm displacement, which can possibly evaluate non-linear soil behaviors. A Balluff displacement sensor (Model BAW-R03) is installed just below the piston to measure the piston movement. A wave spring, sited between the piston and the main blade body, helps keep the piston in line with the blade surface at rest condition. It is noted that, in addition to the chamber housing the piston, displacement sensor, and wave spring, there is a second chamber at the end of the blade opposite to the blade tip. This second chamber is configured to house circuitry and to provide space during assembly and maintenance. O-rings, lodged in the specifically dimensioned grooves, assure a watertight contact between different parts. With the M3 bolts going through the clearance holes and the corresponding nuts fitting the pockets on the other side of the blade, the two removable covers are fixed to the blade. In this way, easily damaged threads in 3D printed materials can be avoided. In addition, the iDMT blade is 15 mm thick, 95 mm wide, and 50 mm long for the lower tapered section of the tip, which is identical to those of the DMT blade and allows the same soil disturbance during probe insertion.

## 3D PRINTING OF THE INSTRUMENTED DMT BLADE

For the purpose of manufacturing a prototype not only used as a visualization model but also as a device to be calibrated and tested, it was decided to use the laser sintering (LS) process in 3D printing technologies to fabricate the blade in alumide, which is a metallic grey, aluminum-filled polyamide 12 powder. During this process, polyamide 12, which has a lower melting point than aluminum, is sintered to produce a solid object. This process is significantly more economical than direct metal laser sintering (DMLS), which needs very high power lasers to work with metal powders (Christopher 2014). Alumide is characterized by its high stiffness among the non-metallic materials used in 3D printing. The main properties of alumide are shown in **Table 1** (EOS 2012).

**Fig. 2** shows the model in an x-ray visual style to show the inside details of the blade, which presents a challenge for traditional subtractive technology to work inside the compact dimensions of the blade, in particular the limited thickness of 15 mm. For instance, the insufficient space of the two chamber openings, as well as the irregular tunnel connecting the chambers, does not allow the use of standard drilling tools during the operation. By comparison, 3D printing does not suffer from any of the geometrical limitations encountered during these traditional processes. Once the 3D model of the iDMT blade is sent to either a desktop LS printer or a professional LS printer, the prototype can be obtained rapidly, within 1 day. However, the desktop LS printer that costs approximately $5,000 appears not to be robust enough to print objects with an accuracy of less than 1.0 mm, which is not satisfactory for the iDMT blade. A professional LS printer with a price tag of about $250,000 can guarantee a better accuracy of ±0.3 % (with a lower limit of ±0.3 mm); nevertheless, users normally do not purchase such a professional printer but request a 3D printing service, so the cost of printing this iDMT blade is around $300. **Figs. 3** and **4** show the separate components of the blade in both the 3D model (up) and the 3D printed result (down). A comparison of the design and the printing product in dimensions as a proof of accuracy is shown in **Table 2**. It is noted that the error in blade thickness is slightly larger than that of other dimensions, which is possibly because of the fact that the model is printed layer by layer in the orientation along the axis of thickness.

## OVERALL INSTRUMENTED DMT SYSTEM

**Fig. 5** demonstrates an overall schematic of the computer control and data-acquisition (DAQ) system for a pressure-controlled test, which can automatically record the measurements and electrically regulate the pressure. The computer control program is developed in Labview (National Instruments); thus, the testing procedure can be controlled in a computer, such as incorporating unload–reload loops and varying loading/unloading rate. Although it would be ideal to measure the pressure near the piston, the pressure sensor is located at

**FIG. 2** Schematic diagram of the instrumented DMT blade in an x-ray visual style.

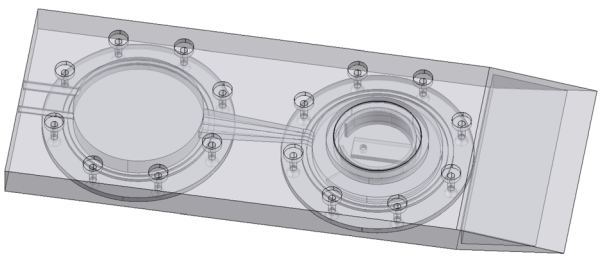

**FIG. 3**

3D printed DMT blade body: (a) bottom view, and (b) top view.

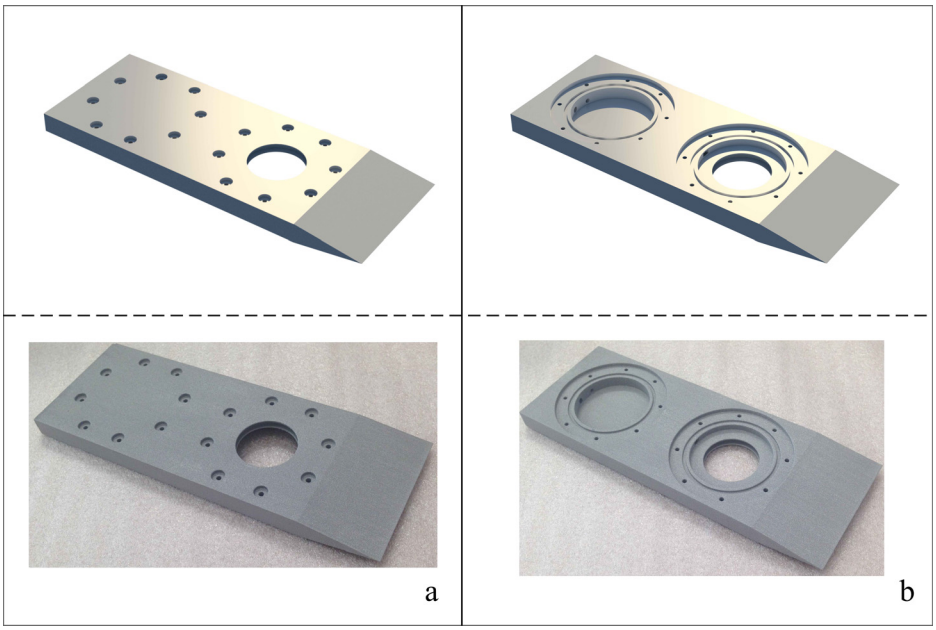


the exit port of the pressure regulator because of the pressure sensor size constraint.

## Calibration

Following the iDMT blade assembly, there are two types of calibration procedures performed in the laboratory. The first procedure involves the piston-displacement calibration and the pressure calibration. As a Honeywell pressure sensor (Model MLH) with a sealed gauge is used with an output from 1 V to 6 V, the pressure calibration is only to determine the zero output at the local temperature and atmosphere.

The piston-displacement calibration is first performed using a Sylvac dial gauge (Model $\mu$233), with an accuracy of 5 $\mu$m and a full range of 12.50 mm, fixed by a custom-built rack to measure the center displacement of the piston. During the

**FIG. 4**

3D printed components of an instrumented DMT blade: (a) removable cover A, (b) piston, and (c) removable cover B.

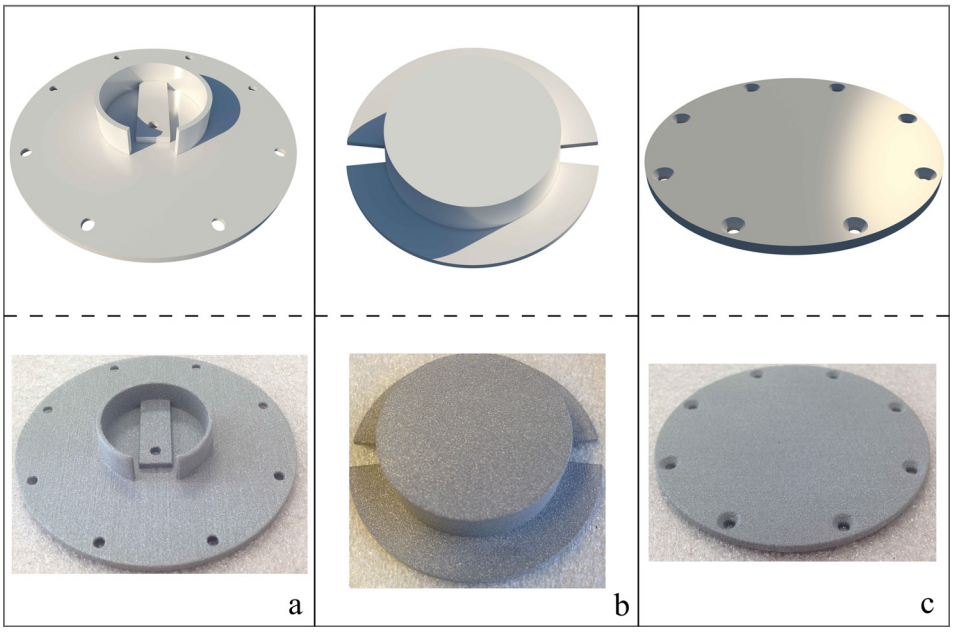

**TABLE 2** Comparison of design and 3D printing dimension.

| | Design Dimension (mm) | Printing Dimension (mm) | Error (%) |
|---|---|---|---|
| Blade width | 95 | 95.77 | +0.81 |
| Blade thickness | 15 | 15.24 | +1.60 |
| Blade length | 260 | 257.92 | −0.80 |
| Piston diameter | 40 | 40.04 | +0.10 |
| Removable cover A diameter | 88.8 | 88.31 | −0.55 |
| Removable cover B diameter | 88.8 | 88.47 | −0.37 |

**FIG. 5**

Schematic diagram of overall instrumented DMT system.

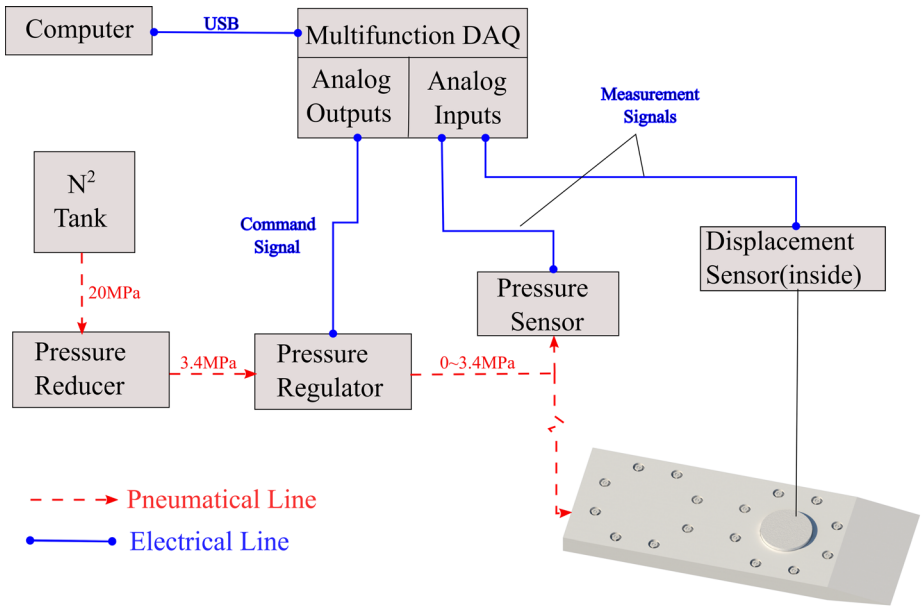


calibration, both the analog voltage output of the displacement sensor and the digital displacement output of the dial gauge were recorded at the same sampling rate. **Fig. 6** shows these measurements up to a displacement of 2.48 mm and a polynomial fit with an adjusted $R^2$ of 0.9997 while the accuracy slightly decreases as it approaches zero and full measuring range.

Then a second calibration is performed in air to determine the force exerted by the wave spring and the friction of the O-ring. This calibration can be useful to obtain the true response of a soil during an in situ test or a calibration chamber test, as the recorded raw pressure-displacement curve includes the wave spring resistance and the O-ring friction. This calibration is preferably carried out both before and after the field test to check the validation. In this calibration, monotonic loading and unloading in air with constant rate is implemented. **Fig. 7** shows pressure plotted against displacement data of two

**FIG. 6** Piston-displacement calibration.

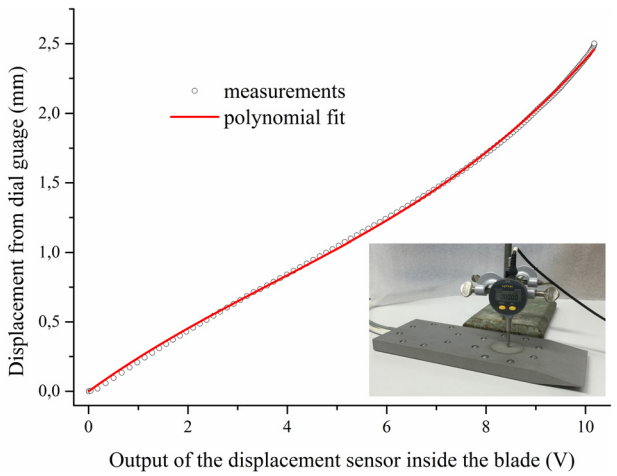

**FIG. 7** Wave spring stiffness and O-ring friction calibration.

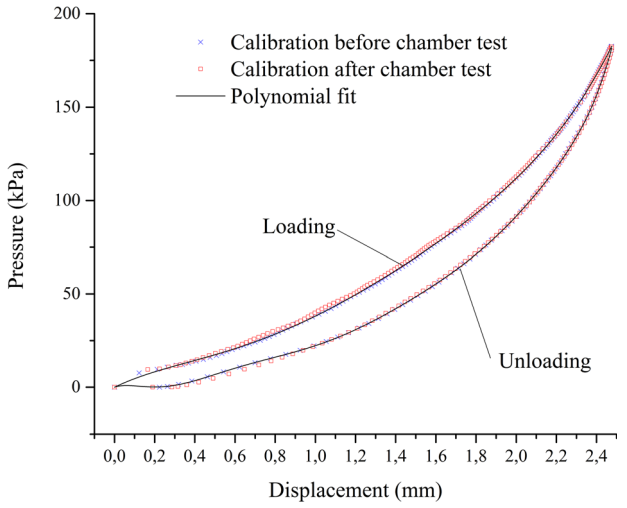


calibrations performed before and after a calibration chamber test. Two polynomial functions were fitted respective to the loading and unloading portion of the calibration data, so a corrected pressure-displacement curve can be produced by subtracting the polynomial functions from the raw pressure-displacement curve.

## Calibration Chamber Testing

### SOIL MATERIAL AND EQUIPMENT

Testing was performed with a dry mol sand sample, which is uniform fine quartz sand with a mean grain size ($D_{50}$) of 0.195 mm, a uniformity coefficient ($C_u$) of 1.60, a maximum void ratio ($e_{max}$) of 0.918, and a minimum void ratio ($e_{min}$) of 0.586 (Karg 2007).

The testing was carried out using the calibration chamber system illustrated in **Fig. 8**. The corresponding boundary condition is zero radial strain, zero bottom strain and zero top stress. It is noted that both blades are wished-in-place to allow a comparison without blade penetration influences, which implies both blades were in place before the sample preparation completed by a pluviation from a bottom sieve of a stationary funnel. The axial symmetrical distribution of the sample and the symmetrical layout of the blades allows a comparison of the results.

### RESULTS AND COMPARISON

The DMT test is performed based on the standard test method without the procedure of penetration (ASTM D6635-01 2007). The membrane calibration is performed three times obtaining consistent results: $\Delta A = 11$ kPa, $\Delta B = 22$ kPa, where $\Delta A$, $\Delta B$ = corrections determined by membrane calibration. However, concerning the DMT test reading $A$-pressure and $B$-pressure: the $A$-pressure is not achieved because of the relatively low soil pressure against the membrane, which is because of the wished-in-place condition of the blade, as well as the relatively low soil pressure in the calibration chamber; the $B$-pressure of 40 kPa is read from the pressure gauge. The iDMT test is conducted in a pressure-controlled model—regulating pressure with a constant rate of 450 kPa/min until the maximum displacement is achieved and decreasing pressure to zero with a constant rate of 900 kPa/min. These pressure rates are specifically valid for the pluviated sand in this calibration chamber and meet the time range of 30 s to 60 s and 15 s to

**FIG. 8**

Calibration chamber system: (a) schematic view, (b) wished-in-place blades during pluviation, and (c) sample preparation completed.

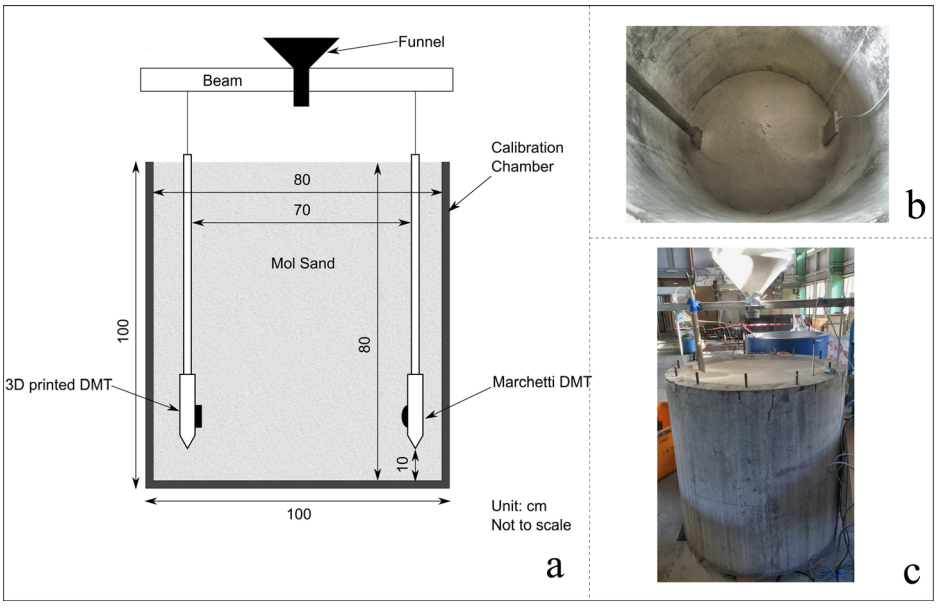

**FIG. 9** Calibration chamber testing results.

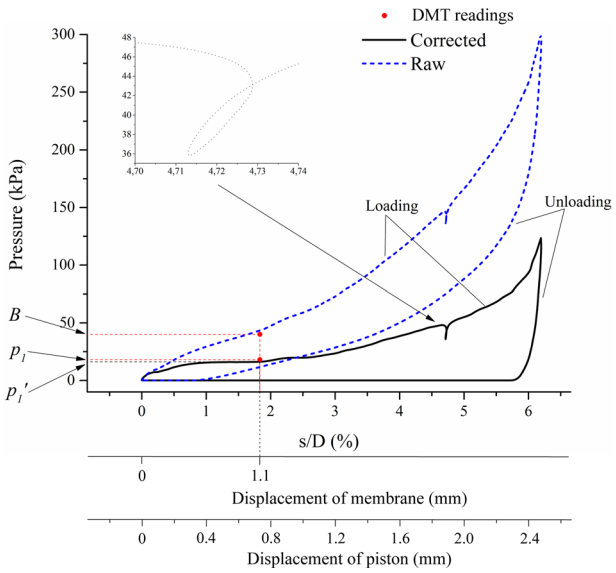


30 s generally required for pressurization and depressurization in a DMT test, respectively. It is noted that the force exerted by wave spring and the friction of the O-ring are critical as they stand for the amount of 60.7 % of maximum total pressure. Because such a large correction is performed, the calibration for determining the force exerted by wave spring and the friction between different parts was repeated after the calibration chamber test. As shown in **Fig. 7**, the repeatability of the two calibration curves is good but with slight deviation in the initial pressure range, and this deviation is within the accuracy range of the pressure sensor: ±8.5 kPa (±0.25 % F.S.). Therefore, it is concluded that the large correction will not cause significant errors in the calculation of the corrected values. **Fig. 9** shows the data from the new iDMT that has a 40-mm diameter piston as well as the standard DMT that has a 60-mm diameter membrane. Thus, to compare the two sets of data, the pressure is not only plotted against the respective *s* but also the normalized *s*/*D*, where *s* is the piston displacement or the membrane center displacement, and *D* is the piston/membrane diameter. As far as the data from the new iDMT is concerned, the corrected curve, which was produced by subtracting the calibration of wave spring resistance and O-ring friction from the raw curve, is shown along with the raw curve. Note that a magnified view of the small unload–reload loop on the corrected curve is also shown. It is seen that the iDMT results are consistent with expectations for a loose sand. During the loading, the soil near the piston is compressed to a denser state and the non-linear pressure-displacement behaviors are mainly caused by the rearrangement of the grains. Because this rearrangement of the grains is irrecoverable on unloading, the soil appears much stiffer in the unload–reload loop than in the loading. Concerning the data from the standard DMT, a $p_1$-pressure is obtained at the membrane displacement of 1.1 mm: $p_1 = B - \Delta B = 18.0$ kPa, and then plotted against an *s*/*D* ratio of 1.83 %. A $p_1'$-pressure of 16.2 kPa is read from the iDMT corrected curve at the same *s*/*D* ratio. The divergence of the two values is acceptable considering the difference in the geometries of loading elements and their corresponding deformation modes. This comparison provides a basic evaluation of the iDMT. Only an approximate comparison can be made between the *A*-pressure that is smaller than the Δ*A* of 11 kPa and a pressure of 5 kPa that is read from the iDMT corrected curve at the same *s*/*D* ratio of 0.083 %. Furthermore, note that 60.7 % of maximum total pressure mainly induced by wave spring resistance is because of the soil pressure in the calibration chamber test not large enough to keep the piston flush with the blade surface at rest condition. In the in situ soil pressure condition that helps return the piston, the correction can be possibly reduced lower than 30 kPa by using a wave spring with lower resistance.

Therefore, with the pressure level of around 268.9 kPa that is produced by subtracting a correction of 30 kPa from the maximum applied pressure of 298.9 kPa during the test, the new iDMT made in alumide shows promise in performing in situ tests at least at shallow depth in soft clay. In case a higher pressure is required, more robust and pricey material such as stainless steel along with DMLS technology shall be used instead of economical alumide together with LS technology.

## Conclusion

This note presents the design and fabrication of an iDMT at UGent, followed by calibrations and a calibration chamber test. The use of 3D printing technology not only successfully completes the iDMT blade fabrication, which cannot be achieved using traditional subtractive manufacturing but also sheds light on using this novel technology in geotechnical testing such as improving laboratory and in situ devices. The use of 3D printing technology allows a larger displacement of the piston to 2.48 mm than that of previous modified DMTs and the standard DMT. Additionally, the use of a computer control and data acquisition system permits the continuous pressure and displacement measurements. With these developments, calibrations and a single calibration chamber test in loose sand have been performed. Preliminary data indicate that the new iDMT has the potential to produce pressure-displacement measurements to a larger strain level than the current standard DMT to evaluate non-linear soil behavior. On the other hand, the testing also proves the feasible use of 3D printed apparatus in soil testing, and the assembled LS products can withstand at least a pressure of 298.9 kPa. This experience may inspire engineers to make potential innovative improvements on geotechnical testing apparatus. The presented work is part of the research in progress on the use of the new iDMT testing, further work will be conducted in situ.

**ACKNOWLEDGMENTS**

This research project is funded by Ghent University and Geosound.be. H.S. acknowledges financial assistance from the program of China Scholarships Council (No. 201306320157). Dr. Benny Malengier is acknowledged for useful comments in 3D printing the iDMT blade. The technicians Filip Van Boxstael and Jan Van der Perre in the Laboratory of Geotechnics at UGent are also acknowledged for their valuable support during the testing.

## References

Akbar, A. and Clarke, B. G., 2001, "A Flat Dilatometer to Operate in Glacial Tills," *Geotech. Test. J.*, Vol. 24, No. 1, pp. 51–60.

ASTM F2792-12a, *Standard Terminology for Additive Manufacturing Technologies*, ASTM International, West Conshohocken, PA, 2012, www.astm.org

ASTM D6635-01, *Standard Test Method for Performing the Flat Plate Dilatometer*, ASTM International, West Conshohocken, PA, 2007, www.astm.org

Campanella, R. G. and Robertson, P. K., 1991, "Use and Interpretation of a Research Dilatometer," *Can. Geotech. J.*, Vol. 28, No. 1, pp. 113–126.

Christopher, B., 2014, *3D Printing*, 2nd ed., ExplainingTheFuture.com, London, pp. 29–81.

Colcott, R. and Lehane, B. M., 2012, "The Design, Development and Application of a New DMT," *Geotechnical and Geophysical Site Characterization 4*, Taylor & Francis, London, pp. 565–570.

EOS, 2012, "Alumide Data Sheet," http://eos.materialdatacenter.com/eo/en (Last accessed 7 June 2015).

Fretti, C., Lo Presti, D., and Salgado, R., 1992, "The Research Dilatometer: In Situ and Calibration Chamber Test Results," *Riv. Ital. Geotech.*, Vol. 26, No. 4, pp. 237–242.

Karg, C., 2007, "Modelling of Strain Accumulation Due to Low Level Vibrations in Granular Soils," Ph.D. thesis, Ghent University, Ghent, Belgium, 132 pp.

Marchetti, S., 1980, "In Situ Tests by Flat Dilatometer," *J. Geotech. Eng. Div.* Vol. 106, No. 3, pp. 299–321.

Marchetti, S., Monaco, P., Totani, G., and Calabrese, M., 2001, "The Flat Dilatometer Test (DMT) in Soil Investigations," *International Conference on In Situ Measurement of Soil Properties*, Bali, Indonesia, May 2001, International Society for Soil Mechanics and Geotechnical Engineering, London, United Kingdom, pp. 95–131.

Schnaid, F., 2009, *In Situ Testing in Geomechanics: The Main Tests*, Taylor & Francis, London, pp. 242–272.

Shen, H., Haegeman, W., and Peiffer, H., 2015, "Instrumented DMT: Review and Analysis," *The 3rd International Conference on the Flat Dilatometer*, Rome, pp. 377–382.

Stetson, K. P., Benoit, J., and Carter, M. J., 2003, "Design of an Instrumented Flat Dilatometer," *Geotech. Test. J.*, Vol. 26, No. 3, pp. 302–309.